

# Growth of vertically aligned carbon nanotubes on carbon fiber: thermal and electrochemical treatments

D. A. L. Almeida · E. F. Antunes · V. Q. da Silva ·  
M. R. Baldan · N. G. Ferreira

Received: 11 December 2012 / Revised: 21 February 2013 / Accepted: 24 February 2013 / Published online: 10 March 2013  
© Springer-Verlag Berlin Heidelberg 2013

**Abstract** Composite electrodes of vertically aligned carbon nanotubes (VACNT) were synthesized on carbon fiber (CF) substrate by pyrolysis of camphor/ferrocene using a SiO<sub>2</sub> interlayer as a barrier against metal diffusion into the substrate. Two treatments were used to remove iron from CF/VACNT structure: thermal annealing at high temperature under inert atmosphere and electrochemical oxidation in H<sub>2</sub>SO<sub>4</sub> solution. The composites were characterized by scanning electron microscopy and Raman scattering spectroscopy. Besides, the electrochemical behavior of CF/VACNT was analyzed by cyclic voltammetry and charge/discharge tests. CF/VACNT composite submitted to the electrochemical oxidation showed the best electrochemical performance, with high specific capacitance, which makes it very attractive as electrode for supercapacitors.

**Keywords** Carbon fiber · Carbon nanotube · Composite · Supercapacitors

## Introduction

The so-called *binderless* carbon-based electrodes have been largely considered in the literature, since they might have a

lower resistance in the absence of a polymeric binder and, moreover present lower cost [1, 2]. Particular interest has been demonstrated for electrodes produced from carbon nanotubes (CNT) grown directly on carbon fibers (CF) [3, 4]. However, it is not easy to obtain vertically aligned CNTs (VACNTs) onto CF. The CNT alignment is strongly related to the density of metal nanoparticles used to nucleate it during the growth process. To form the nanoparticles on CF at standard temperatures of CNT production (600–1,000 °C) it is necessary the use a ceramic interlayer as a barrier against metal diffusion into the substrate. Some authors have suggested the use of amorphous-Si [5], SiO<sub>2</sub> [6], or Al<sub>2</sub>O<sub>3</sub> [7] coatings, deposited by plasma or by sol-gel techniques.

The great interest in using the carbon nanotubes (CNTs) in several applications has been motivated by their nanometer dimensions, high specific surface area, and excellent electronic semiconductivity and conductivity [8]. Thus, porous carbon materials with controlled pore size on the nanometer scale and high specific area are very attractive for supercapacitor applications [9]. In this context, the CF coating with VACNT is essential to obtain a composite material with high surface area and good electrochemical properties. The electrode area is related to the required capacitive effect in alternative power sources [10]. Besides, the alignment of CNTs on an electrode promotes the reduction of the internal electric resistance, which improves the transfer electron process due to the decrease of the ion pathway during the charge/discharge measurements [9].

According to the literature, the specific capacitance of electric double layer capacitors made from CNTs is not very high. The value presented in organic electrolyte is only about 20–30 F g<sup>-1</sup>. However, it can replace other materials formed from carbon because of their nanometer dimensions hollow tube structure, the electrical conductivity, and excellent chemical

D. A. L. Almeida (✉) · V. Q. da Silva · M. R. Baldan ·  
N. G. Ferreira  
Laboratório Associado de Sensores e Materiais,  
Instituto Nacional de Pesquisas Espaciais—INPE, Av.,  
dos Astronautas 1758, Jd da Granja, 12227-010,  
São José dos Campos, São Paulo, Brazil  
e-mail: dalva.dri@gmail.com

E. F. Antunes  
Universidade Federal de São Paulo—UNIFESP, Rua Talim,  
330 - Jd Aeroporto, 12231-280, São José dos Campos,  
São Paulo, Brazil

stability. According to the literature, to obtain higher specific capacitance, the important factors are the specific surface area of the electrode materials and the electrolyte [11]. In addition, Kim et al. have also reported that the pore size of the carbon material has a significant effect on the capacitive behavior of the electrode, i.e., porous carbon (between 2 and 50 nm) contributes for the best performance of the electrodes [9]. Thus, when the CNTs are oxidized with  $\text{CO}_2$ , this value increase about two times [12], which may be associated with the surface area increase. Another proposed strategy to improve the CNTs specific capacitance has been the use of electrochemical treatment. Liu et al. observed that this treatment promoted two important effects: the CNTs purification by removing the residual particles remain by the catalyst as well as the increase of their mesopore diameters [13].

In this work, we present a way to obtain the CF/VACNT composites using thermal chemical vapor deposition technique from camphor/ferrocene pyrolysis. Two procedures were used to grow VACNT on CF. Firstly; the VACNT was grown directly on CF substrate. Secondly, the samples were produced using the amorphous- $\text{SiO}_2$  layer as a diffusion barrier from the impregnation of CF with tetraethyl-orthosilicate (TEOS), which induced the aligned growth of the CNTs. Thus, two pretreatments were used to remove iron from VACNT/CF structures: thermal annealing at high temperature under inert atmosphere (up to 1780 °C), and electrochemical oxidation in  $\text{H}_2\text{SO}_4$  solution. By comparison, the samples were analyzed by scanning electron microscopy (SEM) and Raman scattering spectroscopy. Charge/discharge curves as well as electrochemical impedance spectroscopy (EIS) were also used to qualify the electrodes and to determine their specific capacitances (farad per gram) before and after the pretreatments.

## Experimental procedure

### Production of carbon nanotubes on CF

The VACNTs were deposited on CF by pyrolysis of camphor/ferrocene at 850 °C, using a  $\text{SiO}_2$  interlayer. Camphor and ferrocene powders were mixed at a proportion of 84:16, vaporized at 200 °C, and then carried to the reaction zone by an inert  $\text{N}_2$  gas flowing at 2 LPM. The  $\text{SiO}_2$  interlayer works as a diffusion barrier against iron diffusion into CF substrate leading to a better formation of catalyst nanoparticles during the deposition process [14]. Thus, this interlayer represents an important experimental step.

A study of  $\text{SiO}_2$  deposition using the TEOS was performed by two different methods: (a) CF impregnation by hydrolysed TEOS and (b) direct impregnation by TEOS. Both impregnations were carried out in liquid phase, and consisted of a simple wetting of CF by either TEOS mixed with water or by pure TEOS. The impregnated electrodes were inserted into the

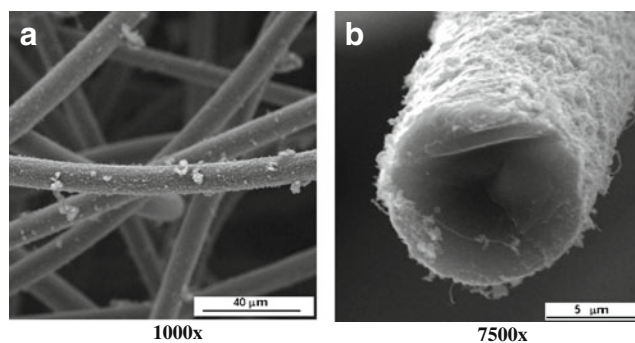


**Fig. 1** a, b CNT grown on pure CF substrate in two different magnifications showing the film around the fibers

reaction zone, and treated at 850 °C for 30 min under  $\text{N}_2$ , prior to VACNT deposition.

A JSM-5310 SEM from JEOL enabled examining the  $\text{SiO}_2$  layers, and the alignment (or not) of the produced CNT films. Raman spectra, recorded from 1,000 to 3,500  $\text{cm}^{-1}$ , by using of a Renishaw 2000 system equipped with Ar laser (514.5 nm), showed the ordering of the CNTs crystalline structures produced on CF substrate.

### Purification of CF/VACNT electrodes by thermal annealing and electrochemical oxidation

Iron inclusions in VACNTs are inherent to their synthesis. Therefore, the electrodes were pretreated before their electrochemical measurements. The CF/VACNT electrodes were treated by two techniques: (1) thermal annealing under  $\text{N}_2$  flow

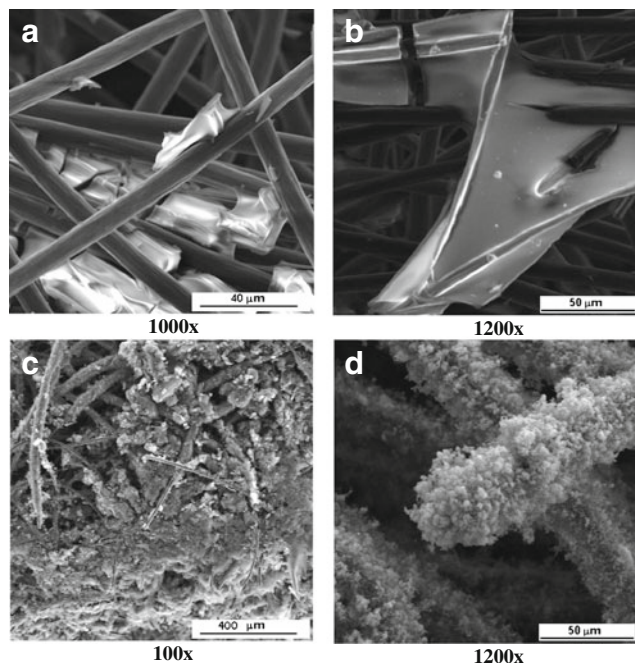


**Fig. 2** SEM images of CF electrodes impregnated by hydrolysed TEOS. a, b  $\text{SiO}_2$  coatings; c, d CNT grown on CF/ $\text{SiO}_2$

at 780 °C for 2 h, and (2) anodic polarization at 1.0 V vs. Ag/AgCl and 3 molL<sup>-1</sup> KCl as supporting electrolyte in solution of 1 molL<sup>-1</sup> H<sub>2</sub>SO<sub>4</sub> from 1 to 12 h [15]. Cyclic voltammetry at a scan rate of 10 mV/s were performed to observe the decrease of Fe oxi-reduction peaks at 0.53 and 0.44 V vs. Ag/AgCl, respectively.

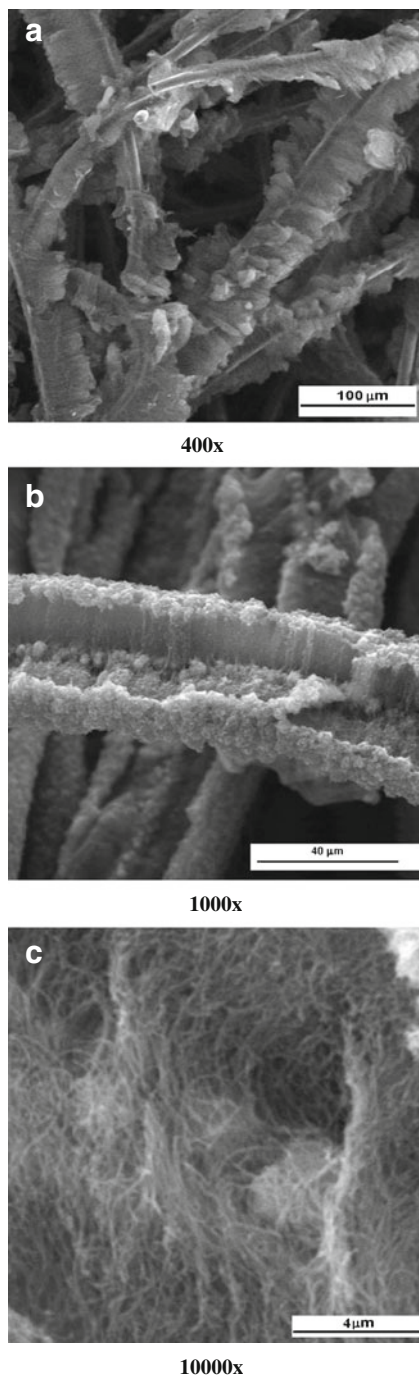


**Fig. 3** SEM images of the CF/VACNT electrodes produced by direct CF impregnation of TEOS in different magnifications. Image (a) shows the fibers completely covered by CNT where the vertically alignment presents better visualization in image (b). Image (c) shows in higher magnification the high CNT density

## Electrochemical measurements

Cyclic voltammetry and charge/discharge curves were performed in 1 mol L<sup>-1</sup> H<sub>2</sub>SO<sub>4</sub> solution at room temperature using a Potentiostat 302 Autolab. The conventional electrochemical cell with three electrodes was used where the CF/VACNT was the work electrode. The counter and reference electrodes were a disk of Pt screen and a Ag/AgCl, respectively. The potential varied between -0.1 and 0.78 V vs. Ag/AgCl for 10 cycles at different scan rates. The capacitance (*C*) is the proportionality coefficient between capacitive current (*i*) and scan velocity (*v*), i.e.,  $i=Cv$ . The capacitances of CF and CF/VACNT electrodes were determined at a scan rate of 10 mV/s. Chronoamperometric tests were performed at 1.0 mA. Charge/discharge curves were used to determine the specific capacitances for all electrodes before and after the pretreatments. The masses of the electrodes were measured before and after the VACNTs growth. The specific capacitance values were calculated taking into account the respective mass for each electrode studied. The Nyquist diagrams were obtained by EIS in a frequency range from 10<sup>-3</sup> to 10<sup>5</sup> Hz with perturbation amplitude of 10 mV.

## Results and discussions

### Production of carbon nanotubes on CF

First of all, we will discuss the VACNT grown on pure carbon fiber, without any pretreatment or diffusion barrier. The SEM images in Fig. 1a, b show the CNT films on such CF substrates. Thin CNT films grew in a heterogeneous way forming clusters and without alignment. To improve the CNT growth, we considered the two methodologies described in the experimental procedure to deposit SiO<sub>2</sub> using TEOS. The method via sol-gel did not provide a good CF covering due to its hydrophobicity. The morphological

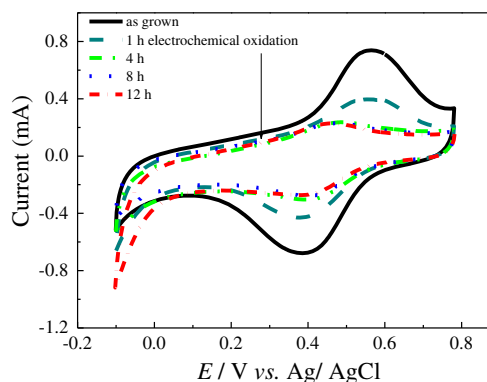


**Fig. 4** Cyclic voltammogram after different periods of electrochemical treatment for samples CF/VACNT

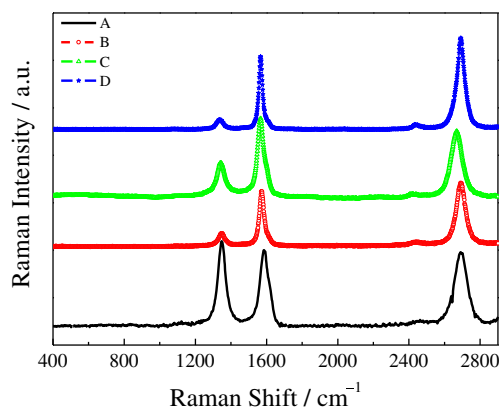


**Fig. 5** Raman Spectra at 514.5 nm for all samples: The indexes (a–d) refer to CF (a), as-grown CF/VACNT (b), oxidized CF/VACNT (c), and annealed CF/VACNT (d)

analyses of this methodology are presented in Fig. 2. Images in Fig. 2a, b show that the CF is not completely wet due to the superficial tension effect between the aqueous solution of TEOS and the fibers. Subsequently, images in Fig. 2c, d depict the CNTs grown on these preceding CF substrates where the films are also heterogeneous forming clusters and thin layers, similar to those presented in Fig. 2a, b images, grown on uncoated CF.

**Table 1** Data obtained from the fitting of Raman spectra for all the samples

Sample	Band	FWHM	ID/IG
CF 1000	D	47.47	1.10
	G	51.51	
	G	85.45	
CF/VACNT as-grown	D	51.03	0.20
	G	31.75	
	G	66.13	
CF/VACNT oxidized	D	63.40	0.43
	G	48.25	
	G	80.20	
CF/VACNT annealed	D	56.84	0.12
	G	24.49	
	G	50.85	

On the other hand, the second methodology used to form the diffusion barrier proved to be very efficient. Figure 3a–c shows CF electrodes coated by CNT grown on SiO<sub>2</sub>, obtained by the direct impregnation of TEOS, followed by pyrolysis at 800 °C. In this case, the CNT grew vertically aligned, and formed a dense forest, demonstrating the effectiveness of the SiO<sub>2</sub> as a barrier against iron diffusion. Particularly, Fig. 3c image depicts the high film density around the fibers.

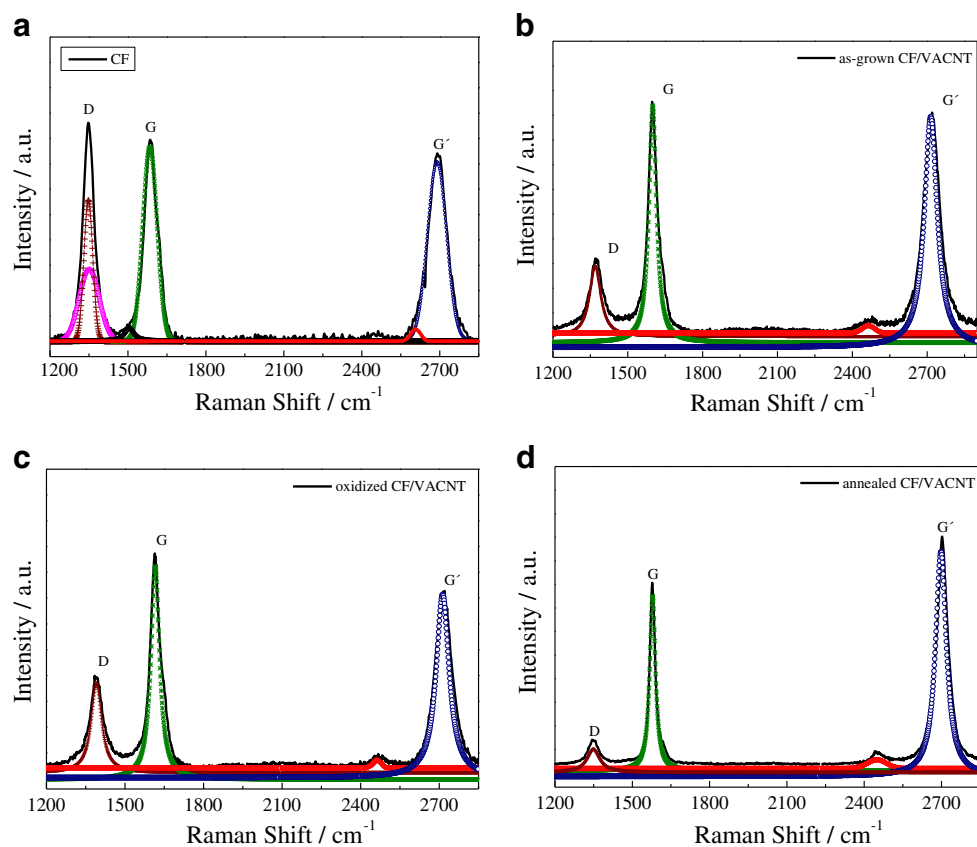


**Fig. 6** Deconvoluted Raman spectra at 514.5 nm for all samples. CF (a), as-grown CF/VACNT (b), oxidized CF/VACNT (c), and annealed CF/VACNT (d)

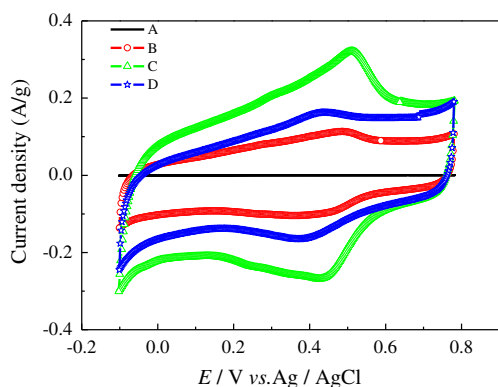


**Fig. 7** Comparative voltammograms of the CF (a), as-grown CF/VACNT (b), oxidized CF/VACNT (c), and annealed CF/VACNT (d). The electrochemical measurements were performed in 1 molL<sup>-1</sup> H<sub>2</sub>SO<sub>4</sub> at 10 mV/s

Purification of CF/VACNT electrodes by thermal annealing and electrochemical oxidation

According to the previous discussion, the subsequent results are presented considering all de VACNT films produced by the

second methodology, using TEOS direct impregnation of TEOS. The literature [14] reported that another form to remove iron ions remaining in CNTs is to maintain an anodic polarization performed in a potential range that includes redox peaks this element. Figure 4 shows the cyclic voltammetry of as-grown CF/VACNT electrodes and after different times of the electrochemical oxidation by anodic polarization at a potential of 1.0 V vs. Ag/AgCl. Figure 4 illustrates one pair of the peaks redox for as-grown CF/VACNT electrodes which can be attributed the presence of the iron. After 1 h of the electrochemical oxidation, a significant decrease of the peaks redox was observed and this was stabilized about 4 h of the treatment. This can be related to a significant removal of the ions Fe in oxidized CF/VACNTs. Figure 5 shows the Raman spectra for all electrodes studied before and after both pretreatments and Fig. 6a–d of the deconvoluted spectra. These results are very important to evaluate the effect of the purification procedures on CF/VACNT atomic structure. The spectra (A–B) refer to CF electrodes before and after the VACNT growth, respectively. Both spectra are graphite-like material [16, 17], and show four main bands: D (~1,352 cm<sup>-1</sup>), G (~1,582 cm<sup>-1</sup>), D' (~1,600 cm<sup>-1</sup>), and G' (~2,700 cm<sup>-1</sup>). Nonetheless, the spectrum (A) is

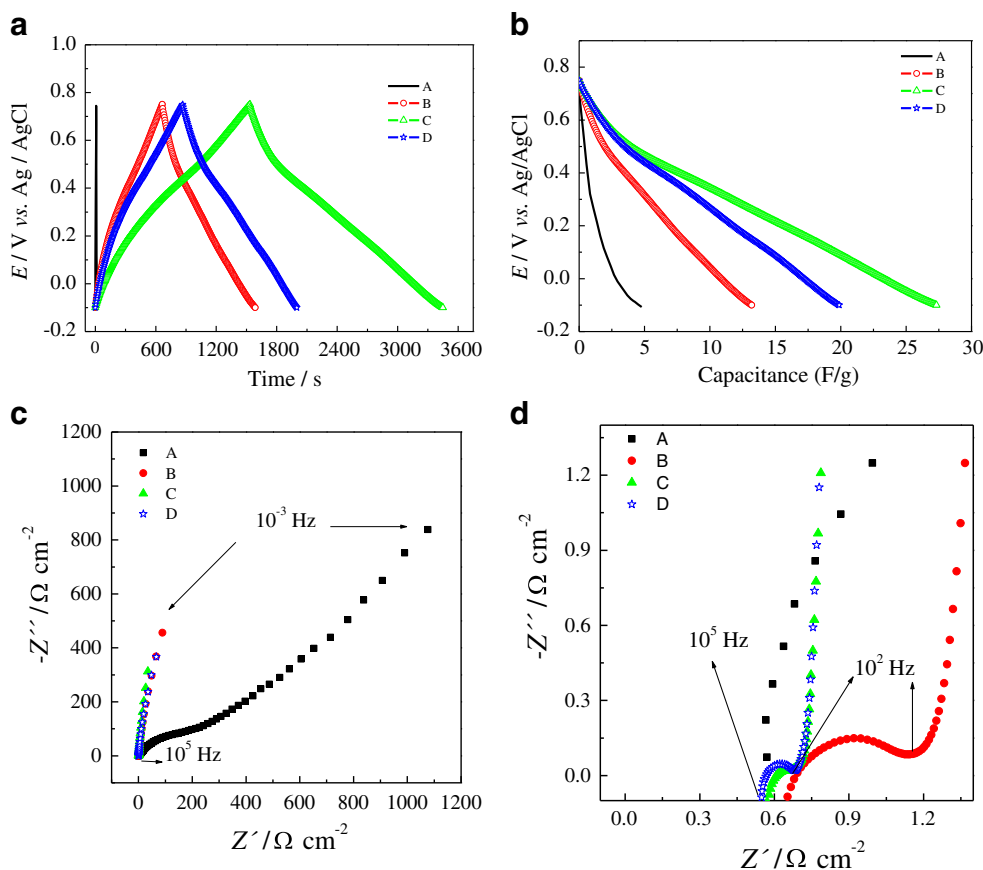


**Fig. 8** a Charge–discharge curves in the potential window range from –0.1 to 0.75 V vs. Ag/AgCl. b Specific capacitance of the electrodes obtained from the charge discharge curves. c Nyquist diagram of CF/VACNT

electrodes, where the curves (d) show details for the Nyquist in low impedance region. The indexes (a–d) refer to CF (a), as-grown CF/VACNT (b), oxidized CF/VACNT (c), and annealed CF/VACNT (d)

compatible with PAN-based CF, i.e., it is the structure of the carbon fibers obtained from polyacrylonitrile precursor graphitized at temperatures around 1,000 °C [18, 19] as expected, while the spectrum (B) shows a D band decrease, characteristic of the CNT structure.

To compare the Raman spectra, some information should be taken into account. The ratio between the intensities of G and D bands ( $I_D/I_G$ ) is used to evaluate the disorder degree of graphitic materials [20, 21]. Considering the four sample types studied (CF, as-grown CF/VACNT, oxidized CF/VACNT, and annealed CF/VACNT), the Raman peaks were fitted by Lorentzian and Gaussian curves to analyze their  $I_D/I_G$  ratios and their full width at half maximum. The complete analysis of the D, G, and  $G'$  bands associated to the  $I_D/I_G$  values are presented in Table 1. In general, VACNT composites show narrower G band compared to that for CF sample. However, the spectrum (C), related to the CF/VACNT after anodic treatment for 4 h (Fig. 5), showed a slight enlargement of the bands in addition to the  $I_D/I_G$  value compared to that for CF/VACNT without treatment. This effect is associated to the disorder increase [22, 23] due to the oxidation process. After

thermal annealing (spectrum D), all the bands became narrower, indicating a better ordering in graphitic structure coated with VACNTs, as expected.

Figure 7 shows the comparative curves of cyclic voltammetry for all samples studied: (A) CF, (B) as-grown CF/VACNT, (C) oxidized CF/VACNT, and (D) annealed CF/VACNT. Clearly, the capacitance of samples coated by VACNTs is much higher than that for pure CF. The capacitance values decreased for the electrodes treated by the thermal annealing since the graphite ordering was improved and the defect density was reduced. Therefore, thermal annealing should be avoided for CF/VACNTs samples purification if they are used as electrodes.

On the other hand, the anodic treatment made the capacitance higher because it oxidizes the electrode surface during the iron removal. This is clearly observed by the broad oxidation peaks around 0.5 V vs. Ag/AgCl that are commonly attributed to a surface redox reaction of oxygen-containing functional groups [9]. Some authors [24, 25] have reported that the oxidation/reduction processes of hydroquinone/quinone groups are responsible for the

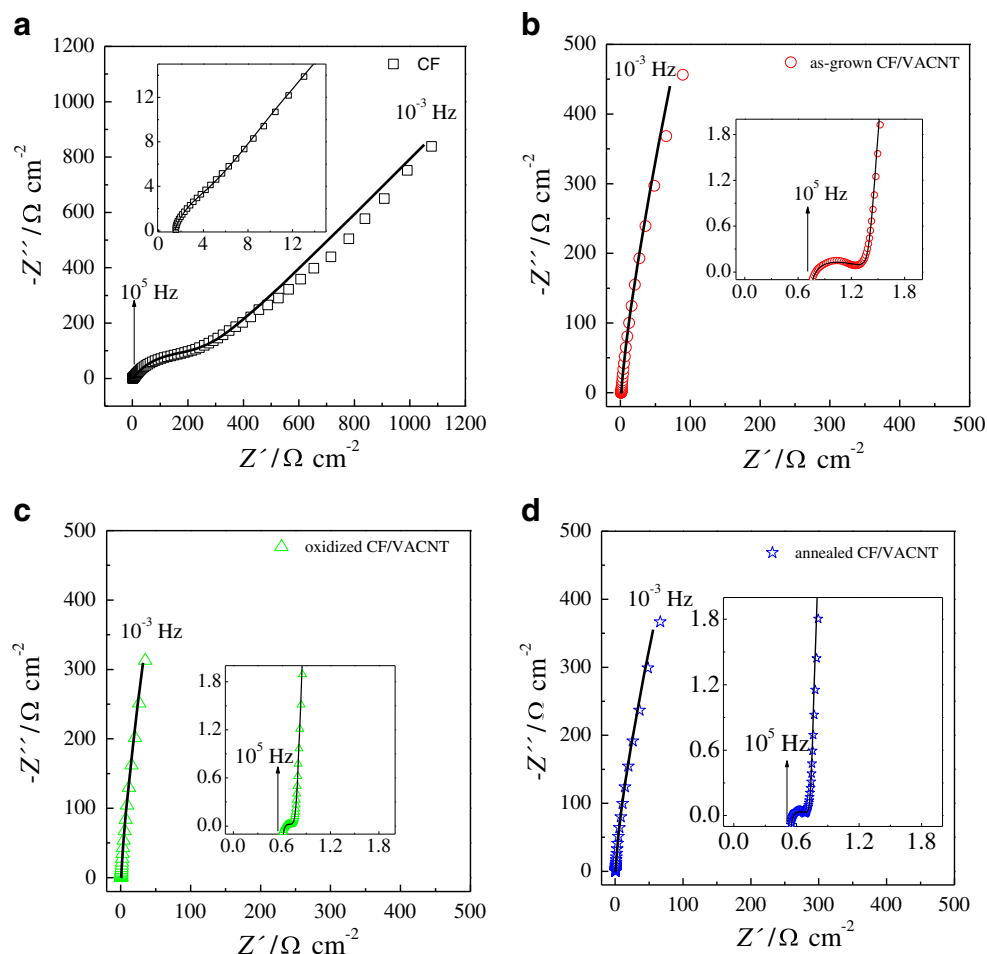
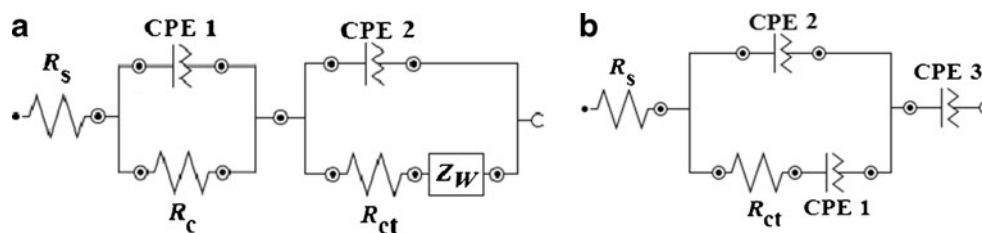


**Fig. 9** Nyquist plots of CF (a), as-grown CF/VACNT (b), oxidized CF/VACNT (c), and annealed CF/VACNT (d). Symbols denote the experimental values while the line represents the fitting of the data to the equivalent circuit in Fig. 10 using the parameters in Table 2

**Fig. 10** Equivalent circuit used to adjust the impedance data (Fig. 9) obtained from the films CF (a), as-grown CF/VACNT (b), oxidized CF/VACNT (c), and annealed CF/VACNT (d) in  $1 \text{ molL}^{-1} \text{ H}_2\text{SO}_4$



majority of the pseudo capacitance measured for carbon materials in acid media, which is related to the appearance of redox peaks. Similar results associated to the capacitance increase due to the oxidation process were also discussed in the literature. Soneda et al. have shown that the oxidation process may open the external layers for multiwall CNT leading to an increase on its surface area [26]. Additionally, some authors have reported an increase on specific capacitance in one order of magnitude after acidic treatment, commonly used for exfoliating graphite [27] or only for activating carbon [13].

**Electrochemical measurements**

The preceding samples were also analyzed by charge/discharge measurements. The charge/discharge curves are shown in Fig. 8a while the specific capacitance values are shown in Fig. 8b. Clearly, the time for CF/VACNT electrode charging after anodic treatment was ~2.4 times higher than that for the as-grown CF/VACNT electrode. Consequently, the specific capacitance followed the same behavior. These results confirm the discussion related to the surface area increase promoted by the acid anodic treatment.

Figure 8c–d shows the Nyquist diagram of (A) CF, (B) as-grown CF/VACNT, (C) oxidized CF/VACNT, and (D) annealed CF/VACNT. All composites showed a semi-circle in high-frequency region. The first extrapolation with the axis related to real part of impedance ( $Z'$ ) was around  $0.6 \Omega$  for all analyzed samples in open circuit potential. However, the second extrapolation, in the end of the semi-circle, also related to the real axis, refers to charge transfer resistance ( $R_{ct}$ ). The composites showed  $R_{ct}$  around 0.5, 0.07, and  $0.15 \Omega\text{cm}^2$  for as-grown CF/VACNT, for oxidized CF/VACNT, and for

annealed CF/VACNT, respectively. It is important to observe that both treatments decreased the  $R_{ct}$ . In the case of the thermal treatment, it promotes two positive contributions to enhance the electrode conductivity. Firstly, the CF as well as the VACNT structural organizations improved at treatment temperature higher than  $1,000 \text{ }^\circ\text{C}$ . Secondly, the thermal treatment removes the iron ions in oxide phase, which may work as a barrier for the  $R_{ct}$ .

Considering the electrochemical treatment, a significant contribution is concerning the increase in the micropores and mesopores of the electrode surface by this anodic process, which allows a better wettability. Consequently, a better interaction followed by a better penetration of electrolyte into the electrode pores [12, 21] may occur. In summary, it is also important to emphasize that the impedance curve showing a vertical line (parallel to  $Z''$ ) in Nyquist diagram represents an equivalent circuit composed of a resistance parallel to an ideal capacitor [28]. Therefore, independently of the pretreatments, the CF/VACNT electrodes are predominantly capacitive in low frequency region, as shown in Fig. 9b [29]. For the CF, the corresponding equivalent circuit is shown in Fig. 10a. This model consists of a serial ohmic resistance. The resistance of the electrolyte bulk is represented by the  $R_s$ , while the  $R_c$  is related with the sum of the resistances particle/particle and pore resistance, and  $Z_W$  corresponds to Warburg impedance (W), similar equivalent circuit was proposed by Obradovic et al. [10]. The capacitance of the CF electrode is represented as constant phase element, CPE 1 while CPE 2 is related to the double layer capacitance producing on the interface of the carbon/electrolyte. According to the equivalent circuit given in Fig. 10b for the electrodes CF/VACNT the CPE

**Table 2** Values of the parameters of equivalent circuit element (Fig. 10) obtained by fitting the EIS

Electrodes	$R_s$ ( $\Omega\text{cm}^2$ )	$R_c$ ( $\Omega\text{cm}^2$ )	$R_{ct}$ ( $\Omega\text{cm}^2$ )	CPE <sub>1,4</sub> $Y_0 \times 10^{-4}$ ( $\Omega^{-1}s^n$ )	$n$	CPE <sub>2</sub> $Y_0 \times 10^{-3}$ ( $\Omega^{-1}s^n$ )	$n$	CPE <sub>3,2</sub> $Y_0 \times 10^{-2}$ ( $\Omega^{-1}s^n$ )	$n$	$Z_W$ $Y_0 \times 10^{-2}$ ( $\Omega^{-1}s^{0.5}$ )
CF	1.20	1.37	269	0.33	0.97	0.55	0.62	–	–	0.51
As-grown CF/VACNT	0.65	–	0.50	95.6	0.56	267	0.98	276	0.17	–
Oxidized CF/VACNT	0.57	–	0.071	160	0.63	420	10.	524	0.15	–
Annealed CF/VACNT	0.53	–	0.15	201	0.6	367	1.0	346	0.5	–

1 is related to the capacitance VACNT/CF substrate. On the other hand, CPE 2 corresponds to the double layer capacitance produced by accumulation of charge on the film interface/electrolyte in parallel to redox pseudocapacitance while CPE 3 is associated with the saturation charge, i.e., the capacitance limit for each material. As can be seen in Table 2 the values of the  $R_{ct}$  decrease after both pretreatments whereas CPE 2 increases considerably.

## Conclusions

It is not an easy task to acquire comparative data to evaluate the specific capacitance of different electrodes because there are several parameters involved in their electrochemical measurements. One imperative contribution discussed in this work was the active electrode surface area of the CF/VACNT composites that significantly enhanced their capacitive responses. The two purification methodologies studied showed important contributions to remove the iron ions. Particularly, the oxidation degree of the carbon materials also proved its influence on the electrochemical measurements mainly when sulfuric acid is used as electrolyte. The anodic treatment made at constant potential showed the best result considering the application of the CF/VACNT electrode as a supercapacitor, where its charging time was improved by ~2.4 times higher than that for the as-grown CF/VACNT electrode. In summary, this work showed a new way to produce vertically aligned CNT onto CF associated to its electrochemical response. Further works should include studies of activation and exfoliation of CNT tips, which certainly will improve the performance of these electrodes without binders for application in energy storage devices.

**Acknowledgments** We would like to thank M.L. Brison by the SEM images. Special thanks to Fundação de Amparo à Pesquisa do Estado de São Paulo FAPESP by the financial support (Process 2009/17584-0)

## References

- Pandolfo AG, Hollenkamp AF (2006) Carbon properties and their role in supercapacitors. *J Power Sources* 157:1–27
- Bordjiba T, Mohamedi M, Dao LH (2007) Binderless carbon nanotube/carbon fibre composites for electrochemical micropower sources. *Nanotechnology* 18
- Firsich DW (1997) Binderless carbon capacitor electrodes produced by polymer pyrolysis. *Electrochem Soc Proc* 96:235–242
- Rosolen JM, Matsubara EY, Marchesin MS, Lala SM, Montoro LA, Tronto S (2006) Carbon nanotube/felt composite electrodes without polymer binders. *J Power Sources* 162:620–628
- Resende VG, Antunes EF, Lobo AO, Oliveira DAL, TravaAiroldi VJ, Corat EJ (2010) *Carbon* 48:3655–3658
- Ly P, Feng Y-y, Zhang P, Chen H-m, Zhao N, Feng W (2011) *Carbon* 49:4665–4673
- An F, Lu C, Guo J, He S, Lu H, Yang Y (2011) *Appl Surf Sci* 258:1069–1076
- Li C, Wang D, Wang X, Liang J (2005) *Carbon* 43:1557–1583
- Kim J-I, Rhee K-Y, Park S-J (2012) *J Coll Interf Sci* 377:307–312
- Obradovic MD, Vukovic GD, Stevanovic SI, Panic VV, Uskokovic PS, Kowal A, Gojovic SL (2009) A comparative study of the electrochemical properties of carbon nanotubes and carbon black. *J Electroanal Chem* 634:22–30
- Weng T-W, Huang W, Lee K-Y (2009) *Vacuum* 83:629–632
- Seo M-K, Park S-J (2010) *Curr Appl Phys* 10:241–244
- Liu CG, Fang HT, Li F, Liu M, Cheng HM (2006) *J Power Sources* 160:758–761
- Antunes EF, Silva VQ, Caetano VEM., Siqueira L, Corat EJ (2012) Growth of carbon nanotube forests on carbon fibers with a SiO<sub>2</sub> interlayer. *MRS Spring Meeting (Boston USA)*
- Antunes EF, Almeida EC, Rosa CBF, Medeiros LL, Pardini LC, Massi M, Corat EJ (2010) Thermal annealing and electrochemical purification of multi-walled carbon nanotubes produced by camphor/ferrocene mixtures. *J Nanosci Nanotechnol* 10:1296–1303
- Antunes EF, Lobo AO, Corat EJ, Trava-Airoldi VJ, Martin A, Verissimo C (2006) Comparative study of first- and second-order Raman spectra of MWCNT at visible and infrared laser excitation. *Carbon* 44:2202–2211
- Dresselhaus MS, Dresselhaus G, Saito R, Jorio A (2005) *Phys Rep* 409:47–99
- TSE-HAO KO (1996) Raman spectrum of modified PAN-based carbon fiber during graphitization. *J Appl Pol Sci* 59:577–580
- Morita K, Murata Y, Ishitani A, Murayama K, Ono T, Nakajima A (1986) Characterization of commercially available Pan (polyacrylonitrile)-based carbon fibers. *Pure Appl Chem* 58:455–468
- Ferrari AC, Robertson J (2000) *Phys Rev B* 61:14095–14107
- Ferrari AC, Robertson J (2001) *Physical Review B* 64:075414-1–075414-13
- Ebbesen TW, Takada T (1995) *Carbon* 33:973–978
- Matthews MJ, Pimenta MA, Dresselhaus G, Endo M (1999) *Phys Rev B* 59:R6585–R6588
- Kinoshita K (1987) *Carbon electrochemical and physicochemical properties*. Wiley, New York
- Andreas HA, Conway BE (2006) *Electrochim Acta* 51:15–21
- Soneda Y, Yamashita J, Kodama M, Kodama H, Hatori H, Toyoda M, Inagaki M (2006) Pseudo-capacitance on exfoliated carbon fiber in sulfuric acid electrolyte. *Appl Phys A* 82:575–578
- Wang G, Ling Y, Qian F, Yang X, Liu XX, Li Y (2011) Enhanced capacitance in partially exfoliated multi-walled carbon nanotubes. *J Power Sources* 196:5209–5214
- Li H, Jixiao W, Chu Q, Wang Z, Zhang F, Wang S (2009) Theoretical and experimental specific capacitance of polyaniline in sulfuric acid. *J Power Sources* 190:578–586
- Frackowiak E, Béguin F (2002) Electrochemical storage of energy in carbon nanotubes and nanostructured carbons. *Carbon* 40:1775–1787